Journal of Physics: Conference Series

PAPER • OPEN ACCESS

Bubble aspect ratio in dense bubbly flows: experimental studies in low Morton-number systems

To cite this article: G Besagni *et al* 2017 *J. Phys.: Conf. Ser.* **923** 012014

Bubble aspect ratio in dense bubbly flows: experimental studies in low Morton-number systems

G Besagni[1], F Inzoli[1], T Ziegenhein[2], H Hessenkemper[2] and D Lucas[2]

[1] Politecnico di Milano, Department of Energy, Via Lambruschini 4a, 20156, Milano
[2] Helmholtz-Zentrum Dresden-Rossendorf e. V. Institute of Fluid Dynamics, 01314 Dresden, Germany

E-mail: giorgio.besagni@polimi.it

Abstract. Almost every modelling approach of bubbly flows includes assumptions concerning the bubble shape. Such assumptions are usually made based on single bubble experiments in quiescent flows, which is far away from the flow field observed in large-scale multiphase facilities. Considering low Morton-numbers and the highly deformable interface at medium and large Eötvös-numbers, the evaluation of the bubble shape in such systems under real flow conditions is highly desirable. In this study, we experimentally evaluate the bubble shape (in terms of aspect ratio), at low Morton-numbers, in different bubble column setups and a pipe flow setup under different operating conditions. The bubble shape in the bubble column experiments were obtained with cameras at Politecnico di Milano and Helmholtz-Zentrum Dresden Rossendorf (HZDR) whereas the shapes in the pipe flows were measured by the ultrafast electron beam X-ray tomography system (ROFEX) at HZDR. In the bubble column experiments almost the same shape is observed; conversely, the shape in the pipe flows distinctly depends on the flow conditions. In conclusion, in bubble columns the assumption of a constant shape regardless of the flow conditions is valid whereas in pipe flows the turbulence and shear rates can be strong enough to deform distinctly the bubbles.

1. Introduction

Bubbly flows are observed in different industrial applications and in multi-phase reactors. The correct design and scale-up of these reactors rely on the precise knowledge of the fluid dynamics at the different scales: maily, the "*reactor-scale*" and the "*bubble-scale*". In particular, at the "*bubble-scale*", the knowledge of the interface size and shape is crucial to characterize the heat and mass transfer phenomena and to model multiphase flows properly. Generally, the bubble shape depends on the fluid dynamic phenomena and the phase properties (viz, the physical and the interfacial properties, as discussed in ref. [1]). On the practical point of view, the bubble shape can be estimated by the aspect ratio (E, the ratio between the minor and the major axes), as discussed by Ellingsen and Risso [2]. Of course, the bubble shape can be related, by the dimensional analysis to non-dimensional groups; for example, the well-known Clift diagram [3] relates the bubble shape to the Morton, the Eötvös and the Reynolds numbers. Another common strategy is to study the influence of the flow phenomena and the phase properties on single bubbles and to apply the obtained models to more complex flows. In this respect, the reader may refer to the literature surveys in refs. [4, 5] and to the discussions in some of the very recent studies [6, 7]. Despite its importance, a comprehensive evaluation of the aspect ratio

under realistic flow conditions (viz. swarm of bubbles) is missing and limited to single bubbles. This study contributes to the existing discussion and it investigates the integral dependencies (i.e., the gas and liquid flow rates, the column design and the sparger setup) on the bubble shape, in low Morton-numbers systems (air-water). To this end, bubble shape data were obtained with cameras at Politecnico di Milano (PoliMI) and Helmholtz-Zentrum Dresden Rossendorf (HZDR); in addition, bubble shapes were measured in pipe flows by using the ultrafast electron beam X-ray tomography system at HZDR.

2. The experimental setups and experimental methods

In this section, the experimental setups and methods are described. It is worth noting that, when analyzing the bubble shape data obtained in the different experimental setups, following the integral approach of the present work, we evaluated the bubbles over the complete flow cross-sections.

2.1. Politecnico di Milano (PoliMI) bubble columns

The experimental facility (Figure 1) is a non-pressurized "*large-diameter*" and "*large-scale*" circular bubble column (inner diameter 0.24 m, height 5.3 m); plese note that the discussion concerning the "*large-diameter*" and "*large-scale*" effects has been proposed in ref. [1]. The bubble column has been tested in the open tube configuration with a spider sparger (sparger openings: d_o = 2-4 mm) and in the annular gap configuration with a pipe sparger (d_o = 3 mm). The gas sparger openings classify the distributor as a "*coarse*" type [1]. Filtered air and deionizer water have been used and their temperatures were maintained constant at room temperature (295 ± 1 K). Experiments have been conducted both in the batch mode and in the counter-current mode (Table 1 summarizes the tested conditions). The photos have been taken using a NIKON D5000 camera (general settings as follow: Nikon 10-24mm lenses, f/3.5; 1/1600s; ISO400; 4288 x 2848 pixels and a spatial resolution of 11.8 pixel/mm). A 500W LED halogen lamp has been used as light source. The measurement location was located at approximately 2.4 m from the gas sparger, which corresponds to the developed region of the two-phase flow. In dense bubbly flows, the three dimensional shape is not accessible with photographic techniques; however, taking into account the discussion in ref. [2], each bubble is approximated and reconstructed by ellipses. The projected bubble size area has been used to calculate the major and minor axes as well as the bubble size (computed as the spherical equivalent diameter of the rotational volume of the projected area). In order to sample the ellipsoidal bubbles, the approach described by Besagni and Inzoli [1] has been applied. It is worth noting that ref. [1] collects, summarizes and extend all our previous studies concerning bubble column flows.

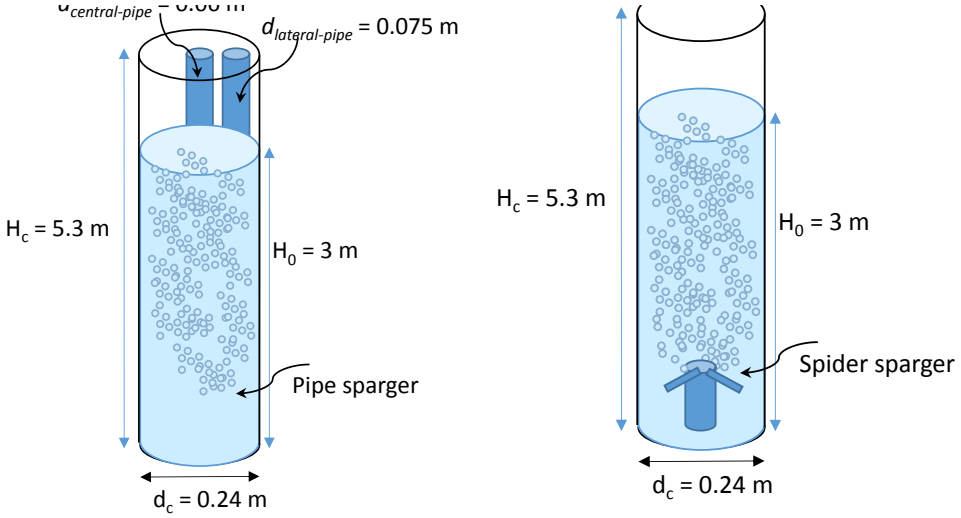

(a) Annular gap bubble column ***(b) Open tube bubble column***

Figure 1. PoliMI bubble column experimental setups.

Table 1. Experimental matrix (PoliMi bubble columns): gas flow rates (U_G) vs. liquid flow rates (U_L).

U_L [m/s] \ U_G [m/s]	0.0037	0.0074	0.0087	0.0111	0.0149	0.0188	0.0220	0.0313
0	*OT*	*OT*	*AG*	*OT*	*OT*	*OT*	*AG*	*AG*
-0.040			*AG*					
-0.066	*OT*	*OT*		*OT*	*OT*	*OT*		

Open tube bubble column (OT), annular gap bubble column (AG)

2.2. Helmholtz-Zentrum Dresden Rossendorf (HZDR) bubble columns

The experimental facilities (Figure 2) are non-pressurized "*small-scale*" and "*small-diameter*" rectangular-section bubble column. Different configurations were tested [8-11]: (a) two "*bubble plume*" experiments (Figure 2a), (b) an airlift reactor (the width of the downcomer is W = 0.06 m; the sparger size varies in the range S = 0.085 - 0.035 m, Figure 2b); (c) a homogenously aerated bubble column (Figure 1c); (d) single needle configuration (the bubble plume setup with one needle in the center); (e) single bubble in different shear flows configuration (single bubbles have been generated in the left side whereas at the right wall many large bubbles rise generating a vortex in which the areas with a linear shear field). The height of the bubble plume and the single needle experiments ranges of H = 0.7 - 0.9 m (Figure 2a); the sparger size varies in the range S = 0.085 - 0.035 m (Figure 2). In Table 2, the inner diameter of the used needles in the sparger (d_o) are shown with the corresponding flow rates. For some experiments, plastic "*caps*" on the needles have been used to generate large bubbles at low flow rates. It is worth noting that the sparger openings classifies the gas spargers ranging from "*fine*" to "*coarse*" type [1]. Filtered air and purified water have been used and their temperatures were maintained constant at room temperature (293 ± 1 K). All experiments have been conducted in batch mode.

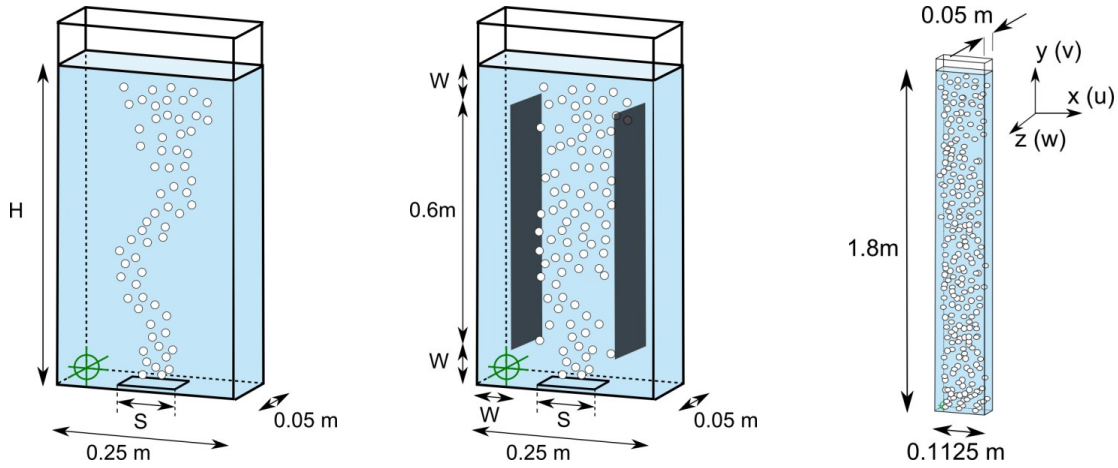

(a) Bubble plume and single needle experiments ***(b) Airlift*** ***(c) Homogenously aerated bubble column***

Figure 2. HZDR bubble column experimental setups.

Bursts of 10 Frames with 400 frames per second have been taken every second by using a Redlake Motion Pro high speed camera (general settings as follow: Samyang 135mm lens; f/5.8; 1/10000 s; 1280x1024 pixels and a spatial resolution of 10 pixel/mm). A 200W LED backlight has been used as light source. The same considerations as reported above (Section 2.1) for the limitations in the photography technique also apply here. For the single bubble experiments the photographs have been evaluated automatically and for all other experiments by hand with support of automated image

analyzes: both techniques are described in refs. [8, 11]. The bubble sizes have been evaluated at different levels in the bubble columns, which have been all sufficiently away from the sparger. Since we have not observed any height dependency of the bubble shape, the results of the different levels were summed up for the single experiments. It is worth noting that, liquid velocity data are available for some of these experimental setup and were discussed by Zieghenein et al. [10, 11]

Table 2. Experimental matrix (HZDR bubble columns): gas flow rates (U_G) vs. inner diameter of the needles (d_o).

d_o [mm]	U_G [m/s]	0	0 - 0.0009	0.0008	0.0024	0.0030	0.0040	0.0053	0.0060	0.0064	0.0071	0.0080
0.12		Single bubble in shear flow	Single needle			Hom						
0.2				BP1	BP1		BP1				Hom	
0.3					BP1	Hom				BP1		
0.5												
0.6						Hom	AL | BP2	BP2	AL			AL
0.7				BP1			BP1			BP1		BP1
0.9						Hom						
1.5					BP1		BP1|BP2	BP2		BP1	Hom	BP1
Caps						Hom						
1.5/0.6							BP2			BP2		

Bubble plume 1 (BP1), bubble plume 2 (BP2), homogenously aerated bubble column (Hom), air lift reactor (AL)

2.3. Vertical pipe experimental setup (HZDR)

The experimental facility is a pressurized "*large-diameter*" and "*large-scale*" vertical pipe (Figure 3a, inner diameter 0.548 m, height 4.95 m). The gas is injected in the lower part of the pipe and flows co-currently with the liquid phase (see ref. [12] for more details). Filtered air and deionizer water have been used; their temperatures and pressures were maintained constant at 303 ± 1 K and 40 bar, respectively. Bubble shape data have been obtained in two flow regimes: the homogeneous flow regime (d_o = 0.8 mm - two conditions tested: (i) U_G = 0.00835 m/s, U_L = 0.405 m/s; (ii) U_G = 0.00835 m/s, U_L = 1.017 m/s) and the slug flow regime (d_o = 1.2 mm - U_G = 0.219 m/s, U_L = 0.405 m/s). Bubble shape information have been obtained, at 3.270 m above the gas sparger (which is the fully developed two-phase flow) by using the ROFEX (*Rossendorf Fast Electron beam X-ray tomograph*) technique. This technique, based on a scanned electron beam approach, was further developed towards a fully operable scanner at HZDR. An electron gun provides an electron beam of 150 kV acceleration voltage and up to 10 kW power. The beam is focused onto a circular X-ray target approximately 1 m away from the gun and is circularly scanned around this target by means of a special electron beam deflection system. The scanner is further complemented by a static circular X-ray detector arranged in the opening inside the scanner head. Fast beam deflection (< 8 kHz), small detector pixels (~1.3 mm pitch) and high read-out frequency (1 MHz) give a high scanning frame rate. Its maximum is 8 kHz but since at that rate spatial resolution deteriorates considerably, scanning speeds up to 2 kHz are used. The measurements were performed in two layers with a distance of 0.102 m to evaluate interfacial velocities. The raw date were processed by a tomographic reconstruction resulting in two stacks of cross-sectional images of the gas volume distribution according to the two measuring layers. A binarisation procedure described by Banowski et al. [13] is applied and single bubbles are identified. By using these data the bubble size distributions as well as bubble shapes are determined. Figure 3b show three-dimensional reconstructed pictures of the flow from ultrafast X-ray tomography measurements, when the time-resolved 2D-Images of the measurement cross-sectional plane get stacked on top of each other.

(a) Experimental setup [13] *(b) Reconstructed 3D-Images of the homogeneous flow regime* *(c) Reconstructed 3D-Images of the slug flow regime*

Figure 3. HZDR pipe flow: experimental setup (a) and post-processing methods (b and c).

3. Experimental results

Herein the experimental results are discussed. First, the influence of the gas and liquid superficial velocities on bubble shape is discussed. Second, the influence of the experimental setup on bubble shape is discussed. Finally, the data are compared with literature correlations. It is worth noting that, the aspect ratio data are generally scattered broadly; therefore, the data are grouped into classes of equivalent diameters. Each class has been represented by the average aspect ratio of the bubbles belonging to that class.

3.1. Influence of the gas and liquid superficial velocity

As discussed by Zieghenein and Lucas [8], the study of the relationships between the aspect ratio E and the gas and liquid superficial velocities provides information concerning if and in which extent the bubble shape is affected when the flow conditions are changed. Nevertheless, with this approach it cannot be determined to which extent local flow values like the shear rate influence the bubble shape. In the worst case, it is possible that different effects are compensated by just increasing the flow rate.

3.1.1. Bubble column experiments

Figure 4 and Figure 5 display the relationships between the aspect ratio E and the gas and liquid superficial velocities for the PoliMi and HZDR (airlift and BP1) bubble columns. The general trend of almost spherical small bubbles and ellipsoidal large bubbles has been observed for all the flow conditions in all the experimental setups. Indeed, in all the experimental setups, a general relationship between the Eötvös number (Eo, related to the bubble size) and E seems to exist: small bubbles have a high aspect ratio, whereas larger bubbles seem to be characterized by lower aspect ratios. Generally, bubbles with equivalent diameters less than 1 mm have an aspect ratio greater than 0.7. This means that the small bubbles tend to be spherical; conversely, bubbles with higher equivalent diameters are characterized by lower aspect ratios (E in the range of 0.4 - 0.7), which reveals the trend of larger bubbles to be flatter. It is also observed that, in all the different experimental setups considered,

changing the gas and liquid superficial velocities does not (generally) influence the bubble shape significantly overall.

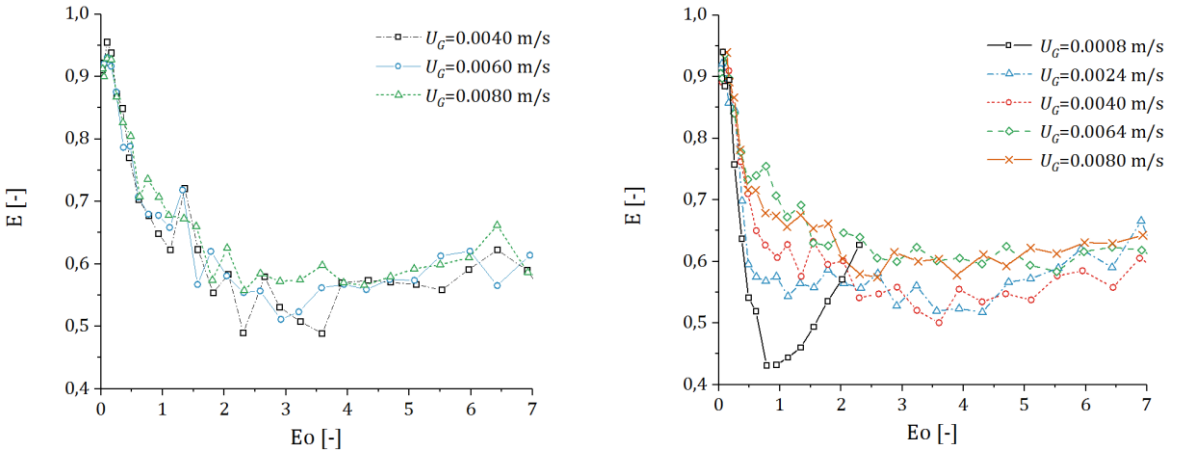

(a) Airlift configuration ***(b) Bubble plume experiment BP1***

Figure 4. Influence of the gas superficial velocity (HZDR bubble columns) on *E* - batch mode.

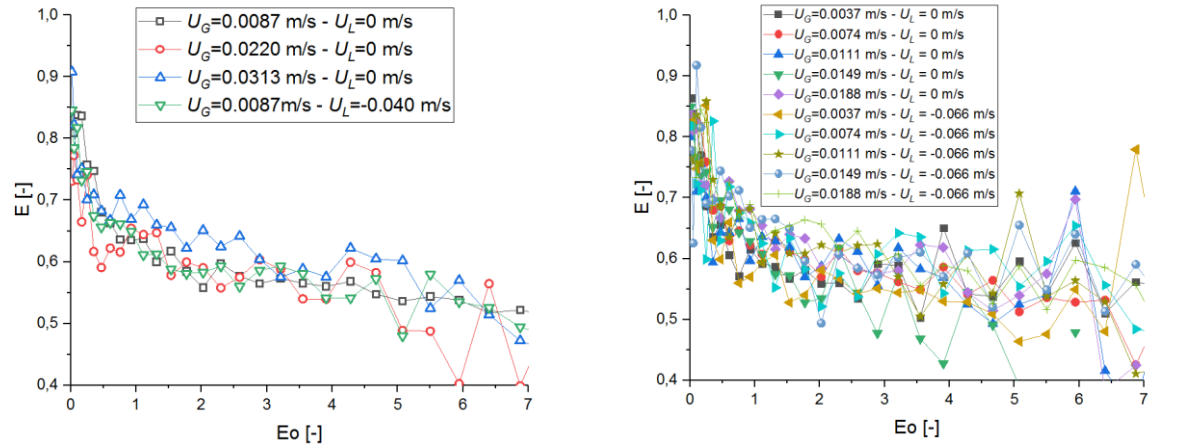

(a) Annular gap bubble column ***(b) Open tube bubble column***

Figure 5. Influence of the gas and liquid superficial velocities on *E* (PoliMi bubble columns).

However, looking closer to the different experimental setups, some additional considerations can be drawn. Considering the airlift configuration (Figure 4a), since the bubble shape is not changing with higher gas superficial velocities, it might be concluded that the bubble shape depends rather on the bubble size distribution and the prevailing flow regime rather than the void fraction (in this respect, see the data and the discussions in ref. [8]). Conversely, the BP1 experiment (Figure 4b) shows a different picture: the aspect ratios increase while increasing the flow rates, and they approach each other for larger bubble sizes. To explain this behaviour, Zieghenein and Lucas [11] compared the flow field of the bubble plume with the airlift reactor; they observed a distinct backflow at the walls with a slightly steeper averaged velocity profile in the airlift configuration; conversely, normal Reynolds stress tensor components ($v'v'$) are similar. The $v'v'$ profiles in the BP1 experiment originate predominantly from the large-scale transient swinging motion of the bubble plume, especially at low gas flow rates. In addition, the bubble size distribution in the BP1 experiment is changing with the flow rates in contrast to a constant bubble size distribution in the airlift reactor for all the flow rates. Since the bubble shape is not changing with higher flow rates in the airlift reactor, it might be

concluded that the bubble shape depends rather on the bubble size distribution and present flow regime than the void fraction for this case (see the discussion in ref. [11]). However, due to the larger bubbles in a wide bubble size distribution, the bubbly flow can be considered "*instable*" (see the lift force discussion proposed in ref. [1]) so that higher local velocity gradients, possible more bubble-bubble interactions, and higher turbulence can be expected. Similar conclusions can be applied to the PoliMI bubble columns in both the batch and in the counter-current mode. It is worth noting that the study of the counter-current mode is interesting, as it produce an additional contribution to the liquid velocity; indeed, in the batch mode the liquid velocity field is completely determined by the recirculation induced by buoyancy counter-current mode. The PoliMI bubble columns are characterised by poly-dispersed bubble size distributions (see, for example, ref. [1], summarizing all our previous studies) that shift towards larger diameters when increasing the gas and liquid superficial velocities (see our previous papers). In the PoliMi bubble columns the bubble shape is not changing with higher gas and liquid superficial velocities, even if the open tube data are more scattered compared with the annular gap data. This observation can be explained considering the higher liquid superficial velocities in the open tube configuration (higher turbulence) and the larger spider sparger openings (resulting in a more poly-dispersed bubble size distribution). Taking into account our other papers focused on the influence of the liquid phase properties [1], we may speculate that the relationship between bubble sizes and shapes (in the homogeneous flow regime) mainly depends upon the system considered (i.e., the liquid phase properties) and not on the flow conditions. This statement has been verified for the PoliMI configuration and its validity to other systems should be checked and verified by means of future studies.

3.1.2. Pipe flow experiments

Figure 6 displays the relationships between the aspect ratio *E* and the gas and liquid superficial velocities for the pipe flow experimental setup. In this case, a larger dependency of the *E* on the flow rates has been observed, if compared with the previously reported experimental results (Section 3.1.1). When considering the data in Figure 6, it is worth noting that, when computing the Eötvös number, beside the bubble size information, physical properties of the air-water system at 303 ± 1 K and 40 bar are needed. It is known that the surface tension is influenced more by temperature than by pressure and, for this reason, it has been estimated based on the data provided in ref. [14].

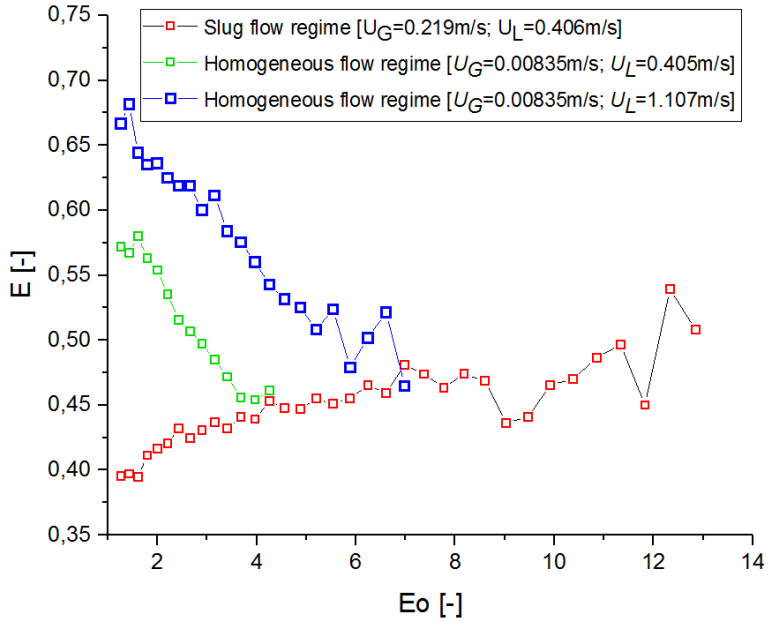

Figure 6. Relationship between *Eo* and E in pipe flows.

When considering the homogeneous flow regime, we observed that (a) E decreases while increasing Eo (larger bubbles tends to be flatter) and (b) E decreases while increasing U_L. It is worth noting that the relationship between E and Eo follows nearly the same trend between the two liquid superficial velocities: increasing U_L, increases the bubble deformation, but the trend does not change. Conversely, the slug flow experiments show a complete different trend: (a) small bubbles are characterised by lower E (b) increasing the bubble size, E increases. These experiments are characterized by a high gas holdup (up to 50 %). Therefore, bubble interactions may have larger influence on the bubble shape as well as wake effects and induced turbulence of larger bubbles. Interestingly, the shape of the smaller bubbles is slightly more influenced by this effect compared to larger bubbles. It is worth noting that pipe flow experiments have bene performed at high U_L; the influence of U_L on the fluid dynamics is probably due to the comparable order of magnitude of the liquid and gas velocities: it is known that if U_L is low compared with the bubble rise velocities, no impact of U_L on the fluid dynamics is expected because the acceleration of the bubbles will be negligible [15, 16].

3.2. Influence of the experimental setup

The conclusion that may be drawn from the previous sections is that in bubble columns the assumption of a constant shape regardless of the flow conditions is valid whereas in pipe flows the turbulence and shear rates can be strong enough to deform the bubble distinctly. In this section, we focus on the influence of the experimental setup on the relationship between E and Eo in bubble column flows. Indeed, besides the influence of the gas flow rate, also the experimental setup determines the flow conditions. In the homogenously aerated column large-scale fluctuations are not dominant, whereas such fluctuations dominate the bubble plume experiments as well as in the PoliMi bubble columns (where further experimental investigation on the liquid local velocities are planned). Inside the riser of airlift reactors, a distinct background flow is observed so that large scales (bubble plume) and small scales are present. The different single-phase background flows, on the other hand, completely determine the single bubble experiments. The single needle experiments can be interpreted as bubble plumes at very low gas flow rates; the bubbles do not ascent in a steady state but might be still less influenced by the background flow. Comparing E of the different experiments, which are averaged over all gas flow rates and needle setups, relatively small but distinct differences can be observed (Figure 7): generally, different aspect ratios are observed in different experimental setups.

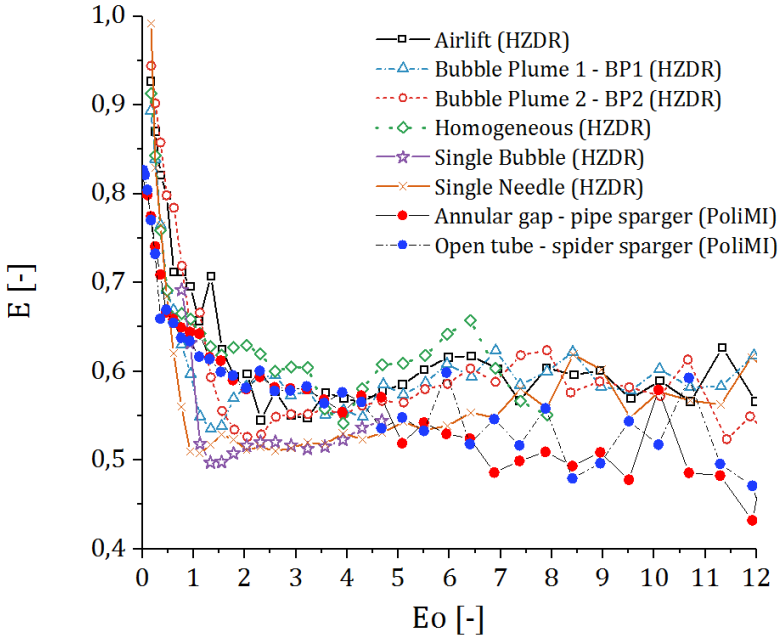

Figure 7. Relationship between Eo and E for the different bubble columns experiments.

The PoliMi bubble column exhibit the smallest aspect ratios for *Eo* > 5 (possibly owing to the very poly-dispersed homogeneous flow regime). Subsequently, the single needle and single bubble experiments exhibit slightly higher aspect ratios compared with PoliMi bubble columns. In addition, the single needle experiment and the single bubble experiment with background flow, however, are almost equal. Interestingly, the aspect ratios measured in the homogenously aerated bubble column are comparable to the aspect ratios observed in these two experiments. In addition, the reproducibility of the experiments is indicated by the almost equal ratios obtained for the two different bubble plume experiments. As would be expected, the aspect ratios observed in the airlift reactor, in which the highest turbulence was measured, are mostly the highest. Generally, distinct differences are observed at smaller bubbles, whereas the aspect ratios approach each other with increasing bubble size.

3.3. Comparison with the literature

Several attempts have been made in the literature to relate the aspect ratio to dimensionless parameters. In this respect, many correlations to relate bubble sizes and shapes were proposed in the last decades; however, most of the studies dealt with single rising bubbles by experimental and numerical approaches and reliable correlations for swarm of bubbles are still not available (see the literature survey in ref. [17] and the analysis of Zieghenein and Lucas [8]). However, when considering dense bubbly flows, these correlations may not be suitable (as deeply discussed by Besagni and Inzoli [1, 17]). The goal of this section is to compare experimental data previously presented and some literature correlations. Detailed studies about the bubble shape from steady state rising single bubbles in quiescent flow can be found in the literature. To compare the results from the present study with these studies, the aspect ratios obtained from the single experimental setups are averaged, thus providing a very large dataset: (a) approximately 7000 and 5000 bubbles in the Polimi open tube and annular gap configurations, respectively; (b) concerning the HZDR experiments, over one million bubbles in the single bubble experiments and around twenty thousand bubbles measured for the airlift experiments. The experimental data have been compared with (a) the fit of Besagni and Inzoli [17] (which has been obtained for dense bubbly flows in annular gap bubble column), (b) the well-known correlation of Wellek et al. [18] and (c) the correlation for super-purified water measured by Sanada et al. [19]. Figure 8 compares the different correlations and the experimental datasets.

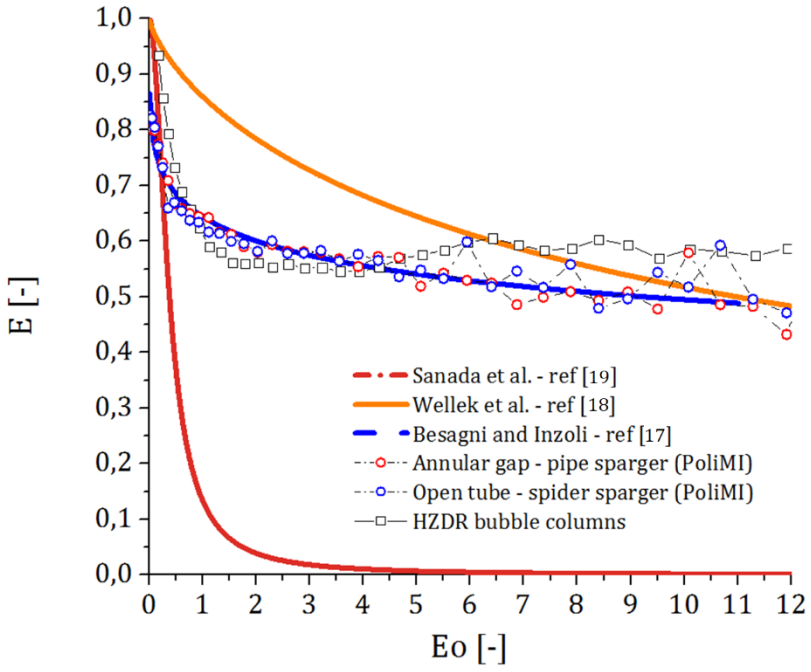

Figure 8. Comparison between literature correlations and aspect ratio experimental data.

The Wellek et al. [18] correlation overestimates the aspect ratio, the Sanada et al. [19] correlation is unable to correlate the aspect ratio; conversely, the correlation proposed by Besagni and Inzoli [17] (obtained for dense bubbly flows) fits the data fairly well. This suggests that correlations taken from the literature should be carefully evaluated before being applied to dense bubbly flows. In future studies, the present dataset should be coupled all together to further improve the scheme of correlation which is under development by some of the authors: indeed, the correlation of Besagni and Inzoli [17], firstly developed for swarm of bubbles in an annular gap bubble column (Figure 1a), has been later modified in a more complex analytical form and has been applied to binary liquid phases to consider active compound systems and viscous liquid phases (see the discussion in Section 4.3.3 of ref. [1]).

4. Conclusions

This paper contributes to the existing discussion concerning the relationships between the bubble shape, size and flow conditions. In particular, we have experimentally evaluated the bubble shapes (in terms of the aspect ratio), at low Morton-numbers, in different bubble column setups and in a pipe flow setup under different operating conditions (representative of real dense bubbly flows). In the bubble column experiments almost the same shape is observed; conversely, the shape in the pipe flows distinctly depends on the flow conditions. Therefore, we may conclude that in bubble columns the assumption of a constant shape regardless of the flow conditions is valid whereas in pipe flows the turbulence and shear rates can be strong enough to deform the bubbles distinctly. In addition, we have demonstrated the importance of developing bubble shape correlations based on data obtained in dense bubbly flows. Future studies will be devoted to extend the present dataset with bubble shape data obtained in binary system and, finally, to propose a general correlation to estimate the bubble shape in real flow conditions.

Acknowledgement

Giorgio Besagni is deeply indebted to Prof. Paolo Di Marco for all the advices and discussions.

References

[1] Besagni G and Inzoli F 2017 *Chem. Eng. Sci.* **170** 270-296
[2] Ellingsen K and Risso F 2001 *J. Fluid Mech.* **440** 235–68
[3] Clift R, Grace J R and Weber M E 1978 *Bubbles, drops, and particles* (New York)
[4] Loth E 2008 *Int. J. Multiphas. Flow* **34** 523-46
[5] Liu L, Yan H and Zhao G 2015 *Exp. Therm. Fluid. Sci.* **62** 109-21
[6] Aoyama S, Hayashi K, Hosokawa S and Tomiyama A 2015 *Exp. Therm. Fluid. Sci.* **79** 23-30
[7] Aoyama S, Hayashi K, Hosokawa S, Lucas D and Tomiyama A 2017 *Int. J. Multiphas. Flow.* **96** 113-122
[8] Ziegenhein T and Lucas D 2017 *Exp. Therm. Fluid. Sci.* **85** 248-256
[9] Ziegenhein T, Zalucky J, Rzehak R and Lucas D 2016 *Chem. Eng. Sci.* **150** 54-65
[10] Ziegenhein T and Lucas D 2016 *Flow. Meas. Instrum.* **48** 36-41
[11] Ziegenhein T, Garcon M and Lucas D 2016 *Chem. Eng. Sci.* **153** 155-64
[12] Banowski M, Beyer M, Lucas D, Hoppe D and Barthel F 2016 *Experiments on vertical gas-liquid pipe flows using ultrafast x-ray tomography* (Technical report HZDR-075, Helmholtz-Zentrum Dresden – Rossendorf)
[13] Banowski M, Lucas D and Szalinski L 2015 *Int. J. Therm. Sci.* **90** 311-22
[14] Vargaftik N B, Volkov B N and Voljak L D 1983 *J. Phys. Chem. Ref. Data* **12** 817-20
[15] Hills J H 1976 *Chem. Eng. J.* **12** 89-99
[16] Rollbusch P, Becker M, Ludwig M, Bieberle A, Grünewald M, Hampel U and Franke R 2015 *Int. J. Multiphas. Flow* **75** 88-106
[17] Besagni G and Inzoli F 2016 *Exp. Therm. Fluid. Sci.* **74** 27-48
[18] Wellek R M, Agrawal A K and Skelland A H P 1966 *AlChE J.* **12** 854–862
[19] Sanada T, Sugihara K, Shirota M and Watanabe M 2008 *Fluid Dyn. Res.* **40** 524-545